Design of a meso-scale high pressure vessel for the laboratory examination of biogeochemical subsurface processes

Authors: Adrienne J. Phillips, Joachim (Joe) Eldring, Randy Hiebert, Ellen Lauchnor, Andrew C. Mitchell, Alfred Cunningham, Lee Spangler, & Robin Gerlach

Phillips, AJ, Eldring, J, Hiebert, R, Lauchnor, E, Mitchell AC, Cunningham, A, Spangler, L, Gerlach, R., "Design of a meso-scale high pressure vessel for the laboratory examination of biogeochemical subsurface processes," Journal of Petroleum Science and Engineering Feb 2015 126: 55–62

Design of a meso-scale high pressure vessel for the laboratory examination of biogeochemical subsurface processes

Adrienne J. Phillips [a,b,n,1], Joachim (Joe) Eldring [a], Randy Hiebert [c], Ellen Lauchnor [a,b], Andrew C. Mitchell [d], Alfred Cunningham [a,b], Lee Spangler [e], Robin Gerlach [a,f,n,2]

[a] *Center for Biofilm Engineering, Montana State University, Bozeman, MT 59717, USA*
[b] *Civil Engineering Department, Montana State University, Bozeman, MT 59717, USA*
[c] *Montana Emergent Technologies, Butte, MT 59701, USA*
[d] *Institute of Geography & Earth Sciences, Aberystwyth University, Aberystwyth, Ceredigion SY23 3DB, UK*
[e] *Energy Research Institute, Montana State University, Bozeman, MT 59717, USA*
[f] *Department of Chemical and Biological Engineering, Montana State University, Bozeman, MT 59717, USA*

Abstract

A meso-scale high-pressure vessel for testing subsurface relevant processes under simulated *in situ* pressures was designed and constructed. This system is capable of providing pressures up to 96 bar and capable of housing porous media samples such as rock cores up to 74 cm in diameter and up to 50 cm high. A valved switchboard allows for fluids to be pumped into and extracted from the vessel and to be sampled in a spatially resolved manner. The switchboard assembly also allows for the monitoring of fluid chemistry in real time, such as pH and conductivity of either the injected or effluent fluids. The vessel can be equipped with an optional heating jacket to control temperatures. The system can be used to investigate a wide range of subsurface relevant processes, including those related to a variety of petroleum industry interests such as fracture sealing for improving the security of geologic carbon sequestration or enhancing wellbore integrity.

As an example, this paper describes the use of the vessel to study ureolysis-driven calcium carbonate precipitation to reduce the permeability of a hydraulically fractured core under relevant subsurface pressure (45 bar). The core was inoculated with *Sporosarcina pasteurii* and biofilm growth was promoted in the fracture, followed by injection of calcium- and urea-containing growth reagents to promote saturation conditions favorable for ureolysis-driven $CaCO_3$ precipitation. This process is referred to herein as microbially-induced calcium carbonate precipitation (MICP). MICP treatment reduced the permeability in the mineralized fracture more than two orders of magnitude. This single high pressure experiment suggests that MICP can be used to reduce permeability in fractures under relevant subsurface conditions. This study also suggests that the high pressure vessel is suitable for testing a range of biogeochemical processes in meso-scale fractured porous media samples under pressure. The high pressure test system could also be well suited for studying microbially-enhanced methane production from coal, wellbore and cement integrity challenges with corrosive fluids, proppant and hydraulic fracturing fluid investigations, enhanced oil recovery, microbially-induced corrosion, or biofouling among many other industry-related biogeochemical processes.

1. Introduction

1.1. Meso-scale investigation of biogeochemical processes

Laboratory studies of geochemical and biogeochemical processes are often limited to the small core scale and may not incorporate reasonable three dimensional and geologic heterogeneity (Yale et al., 2010b). Field tests are expensive, laborious and often field opportunities are limited. Therefore, to prepare for field scale experiments or technology deployment it is important to study *in situ* processes at intermediate scales. Intermediate or

meso-scale experiments (defined here as ~1/2 m to 1 m scale) can more closely simulate real-world environments by incorporating larger scale phenomena that are not captured with typical lab scale experiments (McCallum et al., 2007) and may provide knowledge valuable in the transition to the field scale (DeJong et al., 2010).

Aside from commercially available core analysis equipment, such as those available from Core Laboratories (Texas, USA), high pressure vessels have been designed and constructed for the study of methane hydrates (Eaton et al., 2007; McCallum et al., 2007; Fitzgerald et al., 2012), sampling and analysis of deep sea microbiology (Bianchi et al., 1999) and a large-scale high pressure vessel for purposes of petroleum industry-related studies (Yale et al., 2010a, 2010b). Additional high pressure research equipment is necessary to advance the understanding of biogeochemical processes such as (1) how microbes and microbial activity is affected by pressure and temperature conditions in the subsurface (Abe et al., 1999; Bartlett, 2002; Spilimbergo et al., 2002; Martin et al., 2013), (2) how chemical reactions are enhanced or inhibited by high pressure and (3) how pressure may impact porous media characteristics such as porosity and permeability (Fatt, 1953; Ali et al., 1987).

To contribute to the equipment available, a meso-scale high-pressure vessel (described herein) was constructed and used to study biogeochemical processes in porous media samples under relevant subsurface pressure conditions. The pressure vessel described in this manuscript can be most closely compared to the Yale et al. (2010a, 2010b) LARGE system. The vessel described here has a lower maximum pressure rating (96 bar compared to 144 bar) and sample size capacity (74 cm diameter compared to 210 cm) than the LARGE system. This vessel is similar to the LARGE system as it allows for the study of porous media samples under radial flow and three dimensional conditions.

The specific design of the vessel was driven by tight cost and laboratory height constraints, while meeting the experimental requirements. The vessel alone was fabricated for under $70,000. Overall constructed system cost including switchboard, fittings, pumps, instrumentation and other accessories was approximately $100,000. The system is equipped with high pressure capable pH and conductivity monitoring instrumentation which makes the vessel well suited for studying biogeochemical processes at elevated pressures. Since the vessel is housed in a university environment it is accessible for collaborations. The vessel was shown in this manuscript to be successfully employed to investigate the use of microbially-induced calcite precipitation (MICP) to seal a fracture in a 29 in (74 cm) diameter sandstone core.

1.2. Microbially-induced calcium carbonate precipitation (MICP)

Microbially-induced calcium carbonate precipitation (MICP), particularly ureolysis-driven MICP, has been studied extensively for a wide range of engineering applications (Phillips et al., 2013a) including enhanced oil recovery (Ferris et al., 1996), improving construction materials (De Muynck et al., 2010; Achal et al., 2011; Dhami et al., 2012), consolidating porous media (Whiffin et al., 2007; DeJong et al., 2011; Stabnikov et al., 2011; Tobler et al., 2012), remediating environmental contaminants (Mitchell and Ferris, 2005; Mitchell and Ferris, 2006; Fujita et al., 2008; Okwadha and Li, 2011; Achal et al., 2012; Lauchnor et al., 2013) and enhancing the storage security of geologically sequestered CO_2 (Dupraz et al., 2009; Mitchell et al., 2010; Mitchell et al., 2013; Phillips et al., 2013b). Ureolysis-driven MICP involves microbes, particularly in an attached form, also known as biofilm, to promote the precipitation of calcium carbonate. The microbes produce the enzyme urease which catalyzes the hydrolysis of urea to form carbonate and ammonium. In the presence of calcium, the hydrolysis of urea can create saturation conditions favorable for the precipitation of calcium carbonate (Stocks-Fischer et al., 1999; Hammes and Verstraete, 2002; Ferris et al., 2003).

$$CO(NH_2)_2 + 2H_2O \rightarrow 2NH_4^+ + CO_3^{2-} \quad (1)$$

$$Ca^{2+} + CO_3^{2-} \leftrightarrow CaCO_3\,(s) \quad (2)$$

Ureolysis-driven MICP was used previously to reduce permeability in a hydraulically fractured Boyles Sandstone core at ambient pressure (Phillips et al., 2013b). It was also shown that ureolysis-driven MICP can occur at elevated pressures such as those encountered at geologic CO_2 sequestration or hydraulic fracturing sites (Cunningham et al., 2013; Mitchell et al., 2013). At the time of this study, MICP treatment of porous media and fractured rock was deployed in several field scale experiments (Fujita et al., 2008; van Paassen et al., 2010; Burbank et al., 2011; Cuthbert et al., 2013). The vessel described in this paper could be useful to researchers seeking to add the dimensions of increased scale, temperature and pressure to their experiments prior to field deployment. Meso-scale experiments performed under relevant subsurface conditions and on a near-wellbore scale allow for the testing of injection strategies, monitoring of the population of microbes, and gathering of data to assist in the transition from the laboratory scale to the field-scale.

1.3. Motivation for investigation

The purpose of this paper is to describe a new high pressure test vessel capable of the examination of biogeochemical processes at the meso-scale under subsurface relevant pressures. Another motivation of the research presented in this paper was to assess the application of ureolytic biomineralization under meso-scale and relevant subsurface pressure and temperature in a laboratory experiment to prepare for a planned field scale experiment. One question related to field relevance which motivated the conditions of the laboratory experiment was whether MCIP processes change significantly at pressures related to field deployment. A field test was planned to use MICP in a fractured formation at the depth of approximately 1120 ft accessed through a well drilled through the Fayette Sandstone formation located at the William Crawford Gorgas Electric Generating Plant near Parrish, Alabama, USA. To illustrate the vessel capabilities and prepare for the field deployment, an experiment was carried out under elevated pressure conditions to study the permeability reduction in a hydraulically fractured sandstone core due to ureolysis-induced calcium carbonate precipitation.

2. Materials and methods

2.1. Vessel design and construction

The pressure vessel was designed to inject and extract pressurized aqueous solutions, supercritical carbon-dioxide, or other fluids including gases into meso-scale porous media samples (such as rock cores) of up to 74 cm diameter and 50 cm height under reservoir relevant pressure and temperature conditions. In order to keep the vessel fabrication cost and weight low the vessel was specified for a maximum allowable working pressure (MAWP) of 96 bar at 43 °C. Since the super-critical point for carbon-dioxide resides at 74 bar and 31.5 °C, this means a differential injection pressure of up to 22 bar over the CO_2 critical pressure can be safely applied. The vessel was designed, fabricated and tested according to ASME standards by Alaskan Copper Works in Seattle, Washington.

The vessel is comprised of a bottom sided blind flange of 132 cm diameter and a flanged shell with an inner diameter of 76 cm and 54 cm height. The bottom blind flange is mounted by means of 28 2 in. – 8 UN × 14 in. studs and heavy hex nuts that are tightened to 270 Nm (Fig. 1b). The flange is sealed against the vessel with a 9.5 mm wide Viton O-ring.

The vessel cap has a round access port at the top with an inner diameter of 20 cm. The access port is covered by a raised blind flange of 42 cm diameter. This raised top blind flange has 12 ports that allow for fluid delivery, sampling and extraction under pressure, as well as for the installation of necessary safety features. The top blind flange is mounted by means of 12 1.125 in. – 8 UN × 5 in. studs and heavy hex nuts with a Class 600 spiral gasket used to seal the flange to the shell.

The dry weight of the vessel is 2925 kg, not including the supporting frame that is mounted to the bottom blind flange. All wetted parts of the vessel were fabricated from 304 stainless steel. In order to reduce cost, the bottom flange was made from SA-105 carbon steel clad with a 12.4 mm thick 304L stainless steel plate. The mass of the vessel's flanged top shell is 1350 kg. A gantry-style overhead crane (Contrax Industries, Neenah, WI) specified to 2000 kg (2 metric tons) is used to lift the top shell, and to load or unload heavy samples.

The pressure vessel configuration, with the flat blind flange at the bottom was dictated by tight height constraints in the laboratory, the need for a frame underneath the vessel that assured safe and easy transportation with a pallet jack and the desired experimental and instrumentation configuration. As such, a flat versus spherical bottom shell was constructed.

2.2. Fluid delivery & sampling system design

The fluid delivery and extraction system (Fig. 1) consists of two ISCO D1000 (1000 ml) positive displacement pumps (Teledyne, Nebraska, USA), a packer assembly (Phillips et al., 2013b), an optional sampling jacket and custom designed valved switchboard. The fluid delivery into or extraction from the vessel can be flow rate or pressure controlled. An optional heating jacket can be applied to the outside of the vessel and fluids in the Isco pumps can be heated through their temperature control jackets should experiments under higher or lower temperature than ambient temperature be desired.

2.2.1. Internal vessel sampling jacket

The system was designed with an optional sampling jacket, although the jacket was not used in the experiment described in this paper. The additional space required for the sampling jacket reduces the maximum allowable porous media sample or core diameter to 71 cm. In the event that a non-homogenous or fractured core specimen is used in the vessel, fluids exiting the core at different locations along the circumference and height may vary in flow velocity or composition. The optional internal fluid sampling jacket was designed to selectively sample fluids from certain regions while under pressure (Supporting Information Fig. S1).

The sampling jacket was manufactured from a 20 ga 304 stainless steel sheet metal rolled into a circular sleeve (JE Soares, MT, USA). The sampling jacket diameter is adjustable by an overlapping section that can be tightened against the sample with hose clamps. Flexible tubing or other seals can be used to seal between the core and the sleeve to partition the sampling regions. Fluids from six individual sampling regions could be extracted through pipe inserted between the sample and sleeve which are connected to a manifold (Fig. 2) and routed to the switchboard. The amount of intermixing between fluids that exit the core, and the fluid used to maintain the required confining pressure, could be reduced by filling the space between the sample and the sampling jacket with porous media such as small gravel or polymer balls.

2.2.2. Valved switchboard

A valved switchboard was designed and assembled in order to allow for convenient and safe switching of fluids to different pathways or functions (see Supporting information Fig. S2a,b and c.). A multitude of operational steps in connection with the experimental process can be exercised with this switchboard, such as (1) filling and venting the packer or vessel, (2) injecting a microbial inoculum, (3) cleaning and purging the system between experimental steps, (4) collecting influent and effluent samples and (5) monitoring real time parameters such as pH and conductivity.

Fig. 1 presents a side/front view of the switchboard together with the connecting pipes that lead to the vessel's top flange. The back view of the valve switchboard is shown to illustrate construction of the switchboard which was assembled from stainless steel piping and 210 bar rated 2 & 3-way stainless steel valves to minimize potential corrosion (Fig. 3) (Swagelok, Idaho, USA). Additional schematics (Supporting information Fig. S2a,b and c) illustrate the system diagrams which were used to construct the valved switchboard assembly to perform certain tasks (such as sample the effluent or influent fluids, Fig. S2a and b, respectively).

2.2.3. Safety and control

Since the vessel can be used to investigate biological or corrosive processes, it is a concern that fouling could impair the

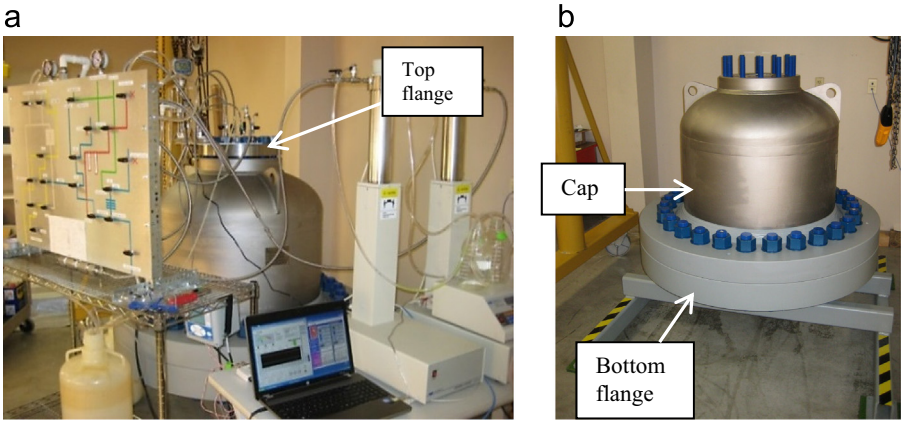

Fig. 1. Meso-scale pressure vessel with fluid delivery and extraction system. (a) Shown on the left is the custom designed switchboard for directing injection fluids, fluid sampling and metering. In the center is the custom fabricated pressure vessel. On the right are two positive displacement pumps (Isco) with controller and a computer for data acquisition; (b) the vessel cap connects to the bottom blind flange by means of 2 in. by 14 in. heavy studs and hex nuts.

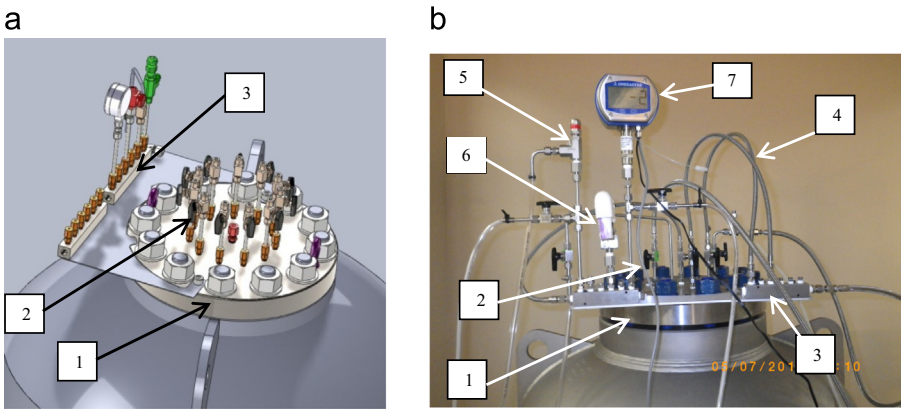

Fig. 2. Top flange manifold illustration and image. (a) Illustration of vessel top flange (1), valve-ports (2) and manifold (3) are connected to each other by way of flexible stainless steel hoses and can be used for sampling, injection and extraction of fluids and connection of safety components; (b) image of the manifold and flexible high pressure hoses (4) connecting the sampling ports from the top flange to the manifold which is connected to the valved switchboard (Figs. 1 and 3). Safety equipment is also shown in (b) including the pressure relief valve (5) burst disk (6) and electronic pressure gauge (7).

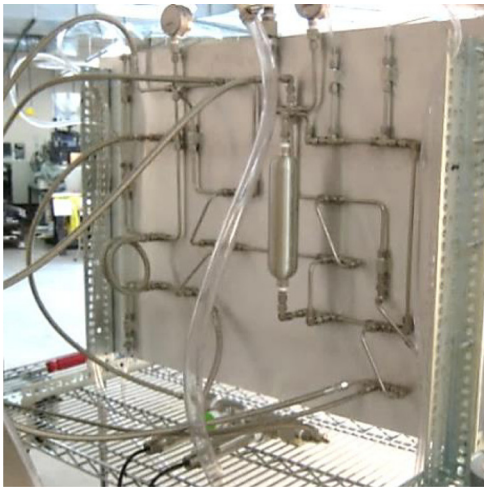

Fig. 3. Image of the valved switchboard system. The back side of the valved switchboard showing the sampling loop (coiled hose to lower left), a reservoir that can be pressurized for injection of inoculum (center-right), and the pH- and conductivity sensors (Barben Analyzer Technologies, Nevada, USA) lying on the wire frame shelf.

function of the safety equipment. To minimize the risk of safety mechanism failure, several redundant safety mechanisms were installed that would be triggered in case of an unacceptable pressure situation including (a) The ISCO/Teledyne pumps are set to not exceed the maximum available working pressure (MAWP); (b) An independently operated pressure sensor (Omega, Connecticut, USA) mounted to the top of the vessel to shut down pump flow in an under- or over-pressure situation combined with electronic notification (e.g., SMS or email) to research personnel; (c) Burst disks (Zook, Ohio, USA) installed in the packer injection piping system and at the vessel; (d) A pressure relief valve set to open at 1400 psi to maintain vessel pressure below MAWP (Swagelok, Idaho, USA).

3. Experimental

3.1. Vessel and core preparation

A Boyles Sandstone core was hydraulically fractured as previously described (Phillips et al., 2013b). Immediately after fracturing, the sandstone core was loaded into the high pressure vessel. A sampling tube was placed directly below the fracture to collect samples of the fluid exiting the fracture (Supporting Information Fig. S3). The vessel was assembled around the core and filled with a 2 g/L NaCl and tap water solution (brine). The core was allowed to saturate over 2 days and the vessel was topped off with brine prior to securing the top flange. Initial fracture permeability was estimated by flowing brine through the packer system, monitoring flow and differential pressure and calculating apparent Darcy permeability based on equations for a confined aquifer in radial flow conditions (Todd and Mays, 2005; Phillips et al., 2013b).

3.2. Fracture sealing experiment

The confining pressure was set to 45 bar by using the Teledyne pump in constant pressure mode to pressurize the brine in the vessel. This pressure was set to mimic relevant subsurface conditions, corresponding to a potential target field deployment site in the Fayette Sandstone layer in Alabama, USA (Richard Esposito, personal communication). Similarly to previously described experiments by Phillips et al. (2013b) and Cunningham et al. (2013), growth medium containing 0.33 M urea was injected into the core via the double packer system prior to injecting a culture of *Sporosarcina pasteurii*. Prior to inoculation, the culture was centrifuged at 3066 *g* (6000 rpm) and re-suspended in fresh growth medium. The culture was then injected through the double packer into the fracture at 20 ml/min. Following a 4.5 h attachment period of no flow, growth medium was injected for 7 h to promote biofilm formation before calcium pulses (0.33 M urea and calcium) were initiated. Calcium pulses were performed as previously described to minimize near-injection-point plugging (Ebigbo et al., 2012; Phillips et al., 2013b). During the experiment, differential pressure and flow rate were monitored to assess changes in permeability over time. Effluent from the sampling region directly below the fracture was monitored in real time to determine changes in chemistry using high pressure pH and conductivity probes (Barben Analyzer Technology, Nevada, USA). Ureolysis was monitored by measuring the increase in conductivity over time, as urea is non-ionic but the products of ureolysis are ionic species (Eq. (1)) (Whiffin, 2004). Additionally, effluent samples were collected during each pulse to determine culturable cell concentrations through drop plate methods (Herigstad et al., 2001) and ammonium production as previously described (Phillips et al., 2013b). In the beginning of the experiment two colony morphologies were observed on the urea-containing agar plates. These colonies were streaked for isolation and the isolated colonies subsequently used to inoculate filter sterilized urea-containing growth medium. Ammonium production and pH were

assessed after 24 h to confirm the two different organisms' potential for ureolysis.

During the first 19 calcium injections, a 24-h cycle was as follows: (1) injection of calcium with a 4 h stagnation period, (2) second injection of calcium with a second 4 h stagnation period, (3) injection of growth medium injection with a 16 h growth period. However, a consistent permeability reduction had not been achieved after calcium pulse #19, which differed from previous ambient condition experiments where the fracture sealed after 14 and 7 calcium pulses in two separate experiments (Phillips et al., 2013b). It was unknown whether the elevated pressure or the presence of confining fluids were impacting the precipitation rates or reducing the efficiency of sealing. Therefore, to compensate for potential negative impacts from pressure or confining fluid conditions, (1) the urea and calcium concentrations of the media were increased to 0.43 M to provide more reactants for precipitation and (2) the 24-h cycle changed to allow more time for biomineralization to occur (1 h of growth medium injection, injection of calcium with a 4–6 h no flow period, then a second injection of calcium and no flow period for 18 h).

The experiment continued until flow rates and differential pressures had reached similar conditions to those observed in previous ambient condition sealing experiments in the same core sample (Phillips et al., 2013b). Since the high pressure vessel does not contain view ports to visualize whether the fracture zone was sealed, permeability was an important metric to evaluating success of the treatment. After reaching the reduced permeability, the vessel was depressurized, confining fluids were drained and the vessel was disassembled for cleaning and maintenance.

Samples of precipitates observed on the outside of the fracture and the inside of the wellbore were collected for analysis including stereoscopy, X-ray diffraction (XRD) and scanning electron microscopy (SEM). Portions of the precipitate samples were ground into a fine powder using an ethanol rinsed mortar and pestle prior to analysis with a X-Ray Powder Diffraction Spectrometer (XRD) (Scintag X-GEN 4000 XRD) at the Image and Chemical Analysis Laboratory (ICAL) at Montana State University. The samples were scanned from 20.0 to 65.0° at 1 °/min and DMSNT analysis software (Scintag) was used to determine mineralogy from the sample spectra. Other portions of the samples were first imaged via stereomicroscopy (Nikon, New York, USA) in the Center for Biofilm Engineering Microscopy Facility and then mounted and coated with iridium for imaging (1 kV) and elemental analysis (20 kV) with a Zeiss Supra 55 Field Emission Scanning Electron Microscope coupled with Energy Dispersive Spectroscopy analysis (Zeiss, Germany) also located in the ICAL.

Finally, the strength of the fracture sealing was determined by (1) applying constant wellbore pressure of 8 bar for 1.75 h and (2) step-wise increasing the applied wellbore pressure (1 bar pressure increase every 2 min) until fluids were observed to be clearly flowing from the fracture.

4. Experimental results and discussion

4.1. Initial apparent Darcy permeability

Prior to starting the fracture sealing experiment the average apparent Darcy permeability of the fracture at a flow rate of brine at 20 ml/min was 26,000 ± 4100 mD.

4.2. Fracture sealing and strength assessment

Urea hydrolysis was monitored in the effluent from the vessel during the calcium and growth pulses by measuring NH_4^+ production and increases in conductivity (Fig. 4a). Over the course of the experiment, NH_4^+ and conductivity on average increased, suggesting active ureolysis was maintained. The initial large jump in conductivity corresponded to an increase in ammonium concentration which immediately followed the biofilm growth stage of the experiment.

During the first three calcium pulses two colony morphologies were observed on plated dilutions of the effluent samples. After isolating the colonies on urea-containing agar, only one of those colony morphologies was observed to be ureolytic. The ureolytic colony morphology was light tan and round, which is typical of the colonies observed in a pure culture of *S. pasteurii*. After the third calcium pulse, only the ureolytic *S. pasteurii*-like organisms were culturable from effluent samples to a high concentration of 2.9×10^7 cfu/ml (Fig. 4b) which is comparable to the maximum population (5.2×10^7 cfu/ml) observed in the effluent of the previously described high pressure experiment (Mitchell et al., 2013). These data suggest that organisms in the non-sterile confining fluids did not out-compete the injected *S. pasteurii* cells. Note: While no other colony morphologies were observed past day three on the aerobic agar plates, anaerobic culturing conditions were not performed and it is possible that anaerobic organisms were present.

An initial reduction in permeability was observed after three calcium pulses, but the reduction was not maintained during an 8 bar, 1.75 h strength test (Fig. 5). After increasing the reagent concentrations and altering the injection strategy to allow for

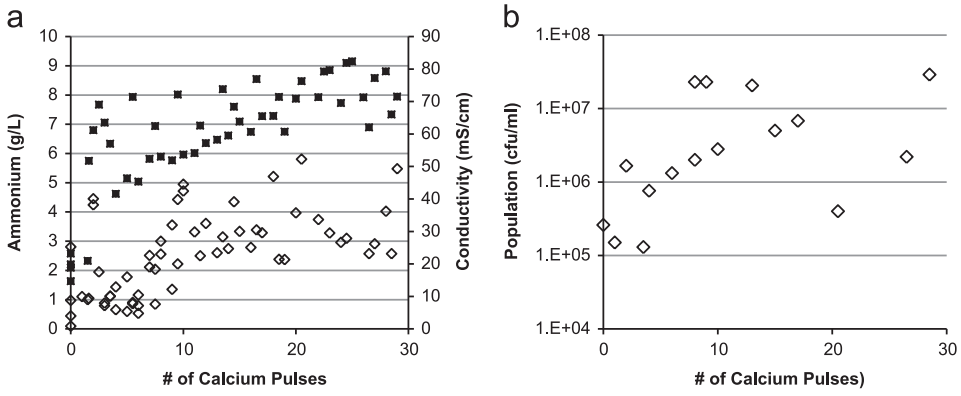

Fig. 4. Effluent ammonium concentrations, conductivity and culturable cell concentrations from vessel effluent samples. (a) Effluent ammonium concentration (◊) and conductivity (■). Ammonium concentration increased from an average of 1.4 g/L ± 1.1 g/L in calcium pulses #1-6 to an average of 3.1 ± 1.1 g/L for calcium pulses #6-28. Conductivity quickly increased from an average of 19.9 ± 2.8 mS/cm to an average of 65.4 ± 10.0 mS/cm after the biofilm growth stage. (b) The culturable effluent population averaged $8.1 \times 10^6 \pm 1.0 \times 10^7$ cfu/ml.

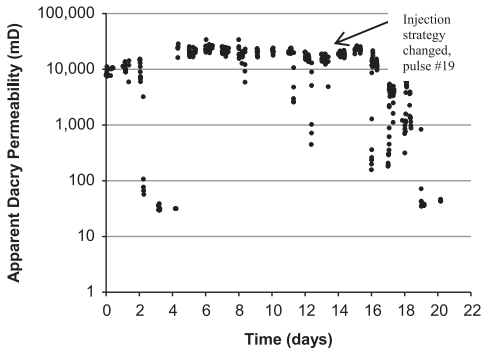

Fig. 5. Calculated apparent Darcy permeability over time (days of experiment). Permeability reduced from approximately 26,000 mD to 40 mD over the course of 21 days and 28 calcium pulses. The injection strategy was altered after 19 calcium pulses (14 days) to increase the concentration of reagents and increase the time allowed for biomineralization.

longer biomineralization periods after calcium pulse #19, the fracture apparent Darcy permeability was observed to decrease (Fig. 5). Previous control experiments resulted in no reduction in permeability when column experiments were pulsed with similar media and tested either without organisms or inoculated with non-ureolytic organisms (Wheeler, 2009). It should be noted that as compared to previous ambient pressure experiments reported in Phillips et al. (2013b), the reduction in apparent Darcy permeability took longer with more calcium pulses in the high pressure system than under ambient conditions (28 calcium pulses instead of 14 and 7 calcium pulses in the two ambient condition experiments) (Phillips et al., 2013b). It is possible that the pressure conditions or the confining fluids themselves impacted ureolysis, yet contrary evidence was reported where high pressure conditions were not shown to negatively impact the kinetics of ureolysis induced by cultures of *S. pasteurii* (Phillips, 2013c). Even so, it is possible the pressure conditions or confining fluids impacted precipitation rates or efficiency. After 28 calcium pulses (21 days post-inoculation) the experiment was terminated as the flow rate and differential pressure had reached 0.3 ml/min and 3.5 bar, respectively, similar to the metrics reached in the ambient pressure sealing experiments and it was assumed the fracture had been sealed.

After the vessel was drained and disassembled, precipitates were observed on the circumference of the core in the region of the fracture and in the wellbore (Fig. 6). SEM and stereoscopy showed the presence of calcium-containing minerals associated with cell-like structures (Supporting Information Fig. S4) and XRD (data not shown) confirmed that the observed minerals were predominantly calcite.

Following mineral sample collection, the fracture was strength tested without confining pressure. First, 8 bar of wellbore pressure was applied for 1.75 h. During this test, flow was observed from the fracture for the first 20 min. After 20 min, no flow was observed from the fracture for the remainder of the 8 bar strength test (Fig. 7). One explanation for the 20 min of observed flow was that even though the fracture itself may have been filled with mineral, residual fluid in the core matrix above and below the fracture flowed toward the circumference of the core due to the pressure field in the wellbore. Another explanation was that depressurization of the vessel damaged the mineral seal and the brine pumped into the fracture during the 8 bar strength test caused loosely bound mineral precipitates to be re-distributed before re-blocking open flow channels.

After 20 min, no flow was observed for the remainder of the 8 bar fracture strength test. Thus after 1.75 h, wellbore pressure was step-wise increased (1 bar pressure increase every 2 min). At a wellbore pressure of 26 bar, fluids were observed to be flowing from the fracture (Fig. 7) indicating re-opening of the fracture. During the re-fracturing event, the flow rate increased rapidly from 4 ml/min at 24 bar differential pressure to 108 ml/min at 26 bar differential pressure. This is similar to the wellbore pressure necessary to re-open the fracture (30 bar and 32 bar) in the two previously described ambient pressure sealing experiments (Phillips et al., 2013b).

5. Summary and conclusions

Here we describe the design and construction of a high pressure vessel, which is capable of housing samples up to 74 cm in diameter and up to 50 cm in height. The vessel is rated to operate at pressures up to 96 bar. The valved switchboard allows fluids to be pumped into the vessel under pressure and radial flow conditions. Sampling of influent and effluent fluids can be accomplished both spatially resolved and under pressure. The system is equipped with real-time monitoring equipment for pH and conductivity. The vessel can be temperature controlled and possesses multiple pressure safety mechanisms.

In an initial experiment, ureolysis-driven microbially-induced calcium carbonate precipitation (MICP) was employed to reduce the apparent Darcy permeability of a hydraulic fracture in a sandstone core under high pressure conditions. The apparent Darcy permeability reduction was attributed to precipitation of calcium carbonate inside the fracture. The final strength of the fracture seal in this single replicate experiment was similar to the strength observed under ambient pressure conditions described previously (Phillips et al., 2013b). This initial experiment also demonstrated some of the capabilities of the meso-scale high pressure vessel such as the use of real-time pH and conductivity monitoring and effluent sampling abilities. The experiment demonstrated that MICP proceeds under pressure conditions similar to those seen at the 1120 ft depth where the Gorgas fractured formation field test was performed. This was significant as the test was performed to better understand how to perform the field experiment and ease the transition from laboratory to field. In the initial laboratory experiment 20 days were required to achieve the desired permeability reduction (fracture sealing); such a long time frame was considered impractical for field deployment. To improve this fracture sealing time, the biomineralization fluid injection strategy was modified by increasing the number of calcium and microbial growth solution pulses per day. This injection strategy modification resulted in a decrease to the overall sealing time required in the field (data not shown).

During the scale-up of new technologies, such as ureolysis-driven MICP treatment of fractures, meso-scale experiments can provide valuable insight. First, reagent concentrations and biomineralization time periods were increased to overcome possibly reduced reaction rates due to an impact from confining fluid or pressure conditions. Field scale conditions may present inhospitable environments to MICP treatment and researchers may have to be prepared to alter injection strategies to overcome those disadvantages to achieve treatment goals. Meso-scale experimental observations can contribute toward the development of effective injection strategies at the field scale.

On a broader scale, this meso-scale high pressure test system can be used to (1) evaluate laboratory-scale developed processes under high pressure and temperature and at larger scale, (2) mimic field scale conditions but with an ability to monitor more parameters than in the field, and (3) study a radial flow configuration which would be similar to a well environment in the field. As technologies progress from the laboratory to the field, meso-scale experiments combined with the use of calibrated models will

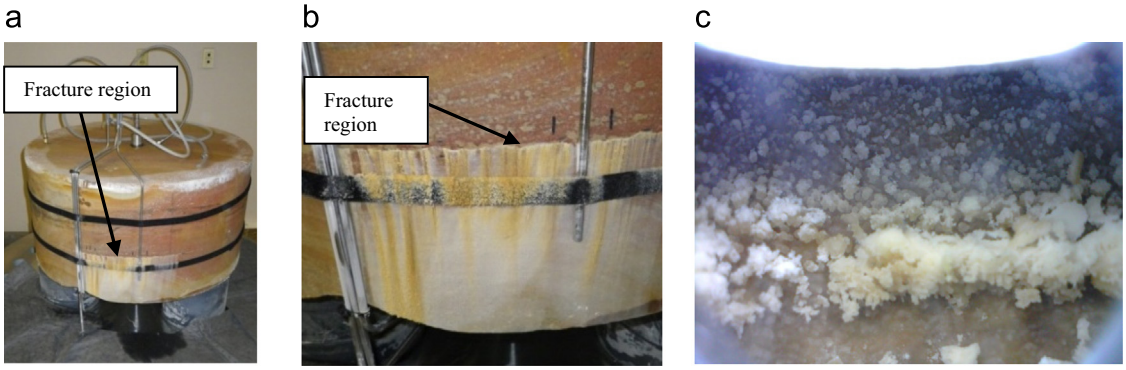

Fig. 6. Precipitates were observed at the end of the high pressure experiment in the region of the fracture. (a) and (b) precipitates formed in the region of the fracture, (c) precipitates were observed inside the simulated wellbore near the elevation of the fracture.

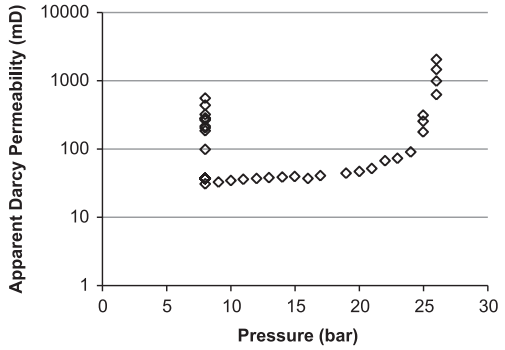

Fig. 7. Calculated apparent Darcy permeability of the fracture during the strength test. Fracture flow was observed in the first 20 min of the 8 bar 1.75 h test, then no flow was observed until the applied wellbore pressure reached 26 bar. At 26 bar of applied wellbore pressure the equivalent permeability increased from ~40 mD to 2500 mD and significant flow was observed from the fracture.

provide valuable resources for successful field applications (Zhang and Klapper, 2010; Barkouki et al., 2011; Fauriel and Laloui, 2011; Wijngaarden et al., 2011; Ebigbo et al., 2012). Future meso-scale experimental investigations will study the effects of supercritical CO_2 on MICP treated fractures, study the ability of MICP to improve wellbore integrity and also study MICP processes under fully radial flow. These experiments will advance the understanding of impacts of pressure and scale on longevity of the permeability reduction created through MICP.

Not only can the vessel be used for MICP related experiments, but the meso-scale high pressure vessel and system components can be adapted to the study of many subsurface processes. Several possibilities include, but are not limited to the study of biologically-induced formation of methane from coal; microbial growth or substrate utilization kinetics under high pressure; microbial community or geochemistry response to supercritical CO_2 injection in formations; methane hydrate investigations; geochemical interactions surrounding hydraulic fracturing; enhanced oil and gas recovery; studies related to unconventional oil and gas recovery; integrity of cement and near wellbore environments after exposure to corrosive environments; microbially-induced corrosion or biofouling and many other industry-related processes.

Acknowledgments

This research was sponsored by two U.S. Department of Energy (DOE) programs: DE-FE0004478, "Advanced CO_2 Leakage Mitigation using Engineered Biomineralization Sealing Technologies" and DE-FE000959, "Field Test and Evaluation of Engineered Biomineralization Technology for Sealing Existing Wells" with matching support from Southern Company and Shell International Exploration and Production B.V. Partial financial support was also provided by DOE DE-FG02-13ER86571 and NSF Award no. DMS-0934696. Any opinions, findings, conclusions, or recommendations expressed herein are those of the authors and do not necessarily reflect the views of the DOE. Partial financial support was also provided from the European Union Marie Curie Reintegration Grant, No. 277005. We acknowledge Shell International Exploration and Production B.V. and Schlumberger Carbon Services for technical advice and oversight. Thanks are extended to engineering researchers Joshua Stringam, Dayla Topp, Neerja Zambare and Adam Rothman. Alaskan Copper (Seattle WA) is acknowledged for their construction and initial testing of the high pressure vessel, as well as for their customer support and attention to engineering details.

Appendix A. Supporting information

Supporting information associated with this article can be found in the online version at http://dx.doi.org/10.1016/j.petrol.2014.12.008.

References

Abe, F., Kato, C., Horikoshi, K., 1999. Pressure-regulated metabolism in microorganisms. Trends Microbiol. 7 (11), 447–453.
Achal, V., Mukherjee, A., Reddy, M.S., 2011. Microbial concrete: way to enhance the durability of building structures. J. Mater. Civ. Eng. 23 (6), 730–734.
Achal, V., Pan, X., Fu, Q., Zhang, D., 2012. Biomineralization based remediation of As (III) contaminated soil by *Sporosarcina ginsengisoli*. J. Hazard. Mater. 201–202 (0), 178–184.
Ali, H.S., Al-Marhoun, M.A., Abu-Khamsin, S.A., Celik, M.S., 1987. The effect of overburden pressure on relative permeability, Fifth Middle East Oil Show. Society of Petroleum Engineers. Manama, Bahrain, pp. 335–341.
Barkouki, T., et al., 2011. Forward and inverse bio-geochemical modeling of microbially induced calcite precipitation in half-meter column experiments. Transp. Porous Media 90 (1), 23–39.
Bartlett, D.H., 2002. Pressure effects on in vivo microbial processes. Biochim. Biophys. Acta (BBA) – Protein Struct. Mol. Enzymol. 1595 (1–2), 367–381.
Bianchi, A., Garcin, J., Tholosan, O., 1999. A high-pressure serial sampler to measure microbial activity in the deep sea. Deep Sea Res. Part I: Oceanogr. Res. Pap. 46 (12), 2129–2142.
Burbank, M.B., Weaver, T.J., Green, T.L., Williams, B.C., Crawford, R.L., 2011. Precipitation of calcite by indigenous microorganisms to strengthen liquefiable soils. Geomicrobiol. J. 28 (4), 301–312.
Cunningham, A., et al., 2013. Abandoned well CO_2 leakage mitigation using biologically induced mineralization: current progress and future directions. Greenh. Gases Sci. Technol. 2, 1–10.
Cuthbert, M.O., et al., 2013. A field and modeling study of fractured rock permeability reduction using microbially induced calcite precipitation. Environ. Sci. Technol. 47 (23), 13637–13643.
De Muynck, W., De Belie, N., Verstraete, W., 2010. Microbial carbonate precipitation in construction materials: a review. Ecol. Eng. 36 (2), 118–136.
DeJong, J.T., Mortensen, B.M., Martinez, B.C., Nelson, D.C., 2010. Bio-mediated soil improvement. Ecol. Eng. 36 (2), 197–210.

DeJong, J.T., et al., 2011. Soil engineering in vivo: harnessing natural biogeochemical systems for sustainable, multi-functional engineering solutions. J. R. Soc. Interface 8 (54), 1–15.
Dhami, N.K., Reddy, M.S., Mukherjee, A., 2012. Improvement in strength properties of ash bricks by bacterial calcite. Ecol. Eng. 39 (0), 31–35.
Dupraz, S., et al., 2009. Experimental approach of CO_2 biomineralization in deep saline aquifers. Chem. Geol. 265, 54–62.
Eaton, M., Mahajan, D., Flood, R., 2007. A novel high-pressure apparatus to study hydrate–sediment interactions. J. Pet. Sci. Eng. 56 (1–3), 101–107.
Ebigbo, A., et al., 2012. Darcy-scale modeling of microbially induced carbonate mineral precipitation in sand columns. Water Resour. Res. 48 (7), W07519.
Fatt, I., 1953. The effect of overburden pressure on relative permeability. J. Pet. Technol. 5 (10), 15–16.
Fauriel, S., Laloui, L., 2011. A Bio-Hydro-Mechanical Model for Propagation of Biogrout in Soils, Geo-Frontiers 2011 Conference. ASCE, Dallas, Texas, USA. pp. 4041–4048.
Ferris, F., Phoenix, V., Fujita, Y., Smith, R., 2003. Kinetics of calcite precipitation induced by ureolytic bacteria at 10 to 20 degrees C in artificial groundwater. Geochim. Cosmochim. Acta 67 (8), 1701–1710.
Ferris, F., Stehmeier, L., Kantzas, A., Mourits, F., 1996. Bacteriogenic mineral plugging. J. Can. Pet. Technol. 35, 56–61.
Fitzgerald, G.C., Castaldi, M.J., Zhou, Y., 2012. Large scale reactor details and results for the formation and decomposition of methane hydrates via thermal stimulation dissociation. J. Pet. Sci. Eng. 94–95 (0), 19–27.
Fujita, Y., et al., 2008. Stimulation of microbial urea hydrolysis in groundwater to enhance calcite precipitation. Environ. Sci. Technol. 42, 3025–3032.
Hammes, F., Verstraete, W., 2002. Key roles of pH and calcium metabolism in microbial carbonate precipitation. Rev. Environ. Sci. Biotechnol. 1, 3–7.
Herigstad, B., Hamilton, M., Heersink, J., 2001. How to optimize the drop plate method for enumerating bacteria. J. Microbiol. Methods 44 (2), 121–129.
Lauchnor, E.G., et al., 2013. Bacterially induced calcium carbonate precipitation and strontium coprecipitation in a porous media flow system. Environ. Sci. Technol. 47 (3), 1557–1564.
Martin, D., Dodds, K., Butler, I.B., Ngwenya, B.T., 2013. Carbonate precipitation under pressure for bioengineering in the anaerobic subsurface via denitrification. Environ. Sci. Technol. 47 (15), 8692–8699.
McCallum, S.D., Riestenberg, D.E., Zatsepina, O.Y., Phelps, T.J., 2007. Effect of pressure vessel size on the formation of gas hydrates. J. Pet. Sci. Eng. 56 (1–3), 54–64.
Mitchell, A.C., Dideriksen, K., Spangler, L., Cunningham, A., Gerlach, R., 2010. Microbially enhanced carbon capture and storage by mineral-trapping and solubility-trapping. Environ. Sci. Technol. 44 (13), 5270–5276.
Mitchell, A.C., Ferris, F., 2005. The coprecipitation of Sr into calcite precipitates induced by bacterial ureolysis in artificial groundwater: temperature and kinetic dependence. Geochim. Cosmochim. Acta 69, 4199–4210.
Mitchell, A.C., Ferris, F., 2006. Effect of strontium contaminants upon the size and solubility of calcite crystals precipitated by the bacterial hydrolysis of urea. Environ. Sci. Technol. 40, 1008–1014.
Mitchell, A.C., et al., 2013. Microbial $CaCO_3$ mineral formation and stability in an experimentally simulated high pressure saline aquifer with supercritical CO_2. Int. J. Greenh. Gas Control 15, 86–96.
Okwadha, G.D.O., Li, J., 2011. Biocontainment of polychlorinated biphenyls (PCBs) on flat concrete surfaces by microbial carbonate precipitation. J. Environ. Manag. 92 (10), 2860–2864.
Phillips, A.J., et al., 2013a. Engineered applications of ureolytic biomineralization: a review. Biofouling 29 (6), 715–733.
Phillips, A.J., et al., 2013b. Potential CO_2 leakage reduction through biofilm-induced calcium carbonate precipitation. Environ. Sci. Technol. 47 (1), 142–149.
Phillips, AJ., 2013c. Biofilm-Induced Calcium Carbonate Precipitation: Application in the Subsurface (Ph.D. thesis). Montana State University (223 pp.).
Spilimbergo, S., Elvassore, N., Bertucco, A., 2002. Microbial inactivation by high-pressure. J. Supercrit. Fluids 22 (1), 55–63.
Stabnikov, V., Naeimi, M., Ivanov, V., Chu, J., 2011. Formation of water-impermeable crust on sand surface using biocement. Cem. Concr. Res. 41 (11), 1143.
Stocks-Fischer, S., Galinat, J., Bang, S., 1999. Microbiological precipitation of $CaCO_3$. Soil Biol. Biochem. 31 (11), 1563–1571.
Tobler, D., Maclachlan, E., Phoenix, V., 2012. Microbially mediated plugging of porous media and the impact of differing injection strategies. Ecol. Eng. 42, 270–278.
Todd, D. and Mays, L., 2005. Groundwater Hydrology, John Wiley and Sons Inc., United States.
van Paassen, L., Ghose, R., van der Linden, T., van der Star, W., van Loosdrecht, M., 2010. Quantifying biomediated ground improvement by ureolysis: large-scale biogrout experiment. J. Geotech. Geoenviron. Eng. 136 (12), 1721–1728.
Wheeler, L.A., 2009. Establishment of Ureolytic Biofilms and their Influence on the Permeability of Pulse-Flow Porous Media Column Systems (Masters thesis). Montana State University, Bozeman, MT (225 pp.).
Whiffin, V., van Paassen, L., Harkes, M., 2007. Microbial carbonate precipitation as a soil improvement technique. Geomicrobiol. J. 24, 417–423.
Whiffin, V.S., 2004. Microbial $CaCO_3$ Precipitation for the Production of Biocement (Ph.D. thesis). Murdoch University, Australia p. 154.
Wijngaarden, W., Vermolen, F., Meurs, G., Vuik, C., 2011. Modelling biogrout: a new ground improvement method based on microbial-induced carbonate precipitation. Transp. Porous Media 87 (2), 397–420.
Yale, D.P. et al., 2010a. Large-Scale Laboratory Testing of the Geomechanics of Petroleum Reservoirs, 44th Annual Rock Mechanics Symposium. American Rock Mechanics Association. Salt Lake City, Utah, USA. pp. 12.
Yale, D.P. et al., 2010b. Large-Scale Laboratory Testing of Petroleum Reservoir Processes, SPE Annual Technical Conference and Exhibition, Society of Petroleum Engineers. Florence, Italy.
Zhang, T., Klapper, I., 2010. Mathematical model of biofilm induced calcite precipitation. Water Sci. Technol. 61 (11), 2957–2964.